

## **Synthesis, characterisation and antibacterial activity of novel Ga(III) polypyridyl catecholate complexes**

Lewis More O'Ferrall, Magdalena Piatek, Brendan Twamley, Kevin Kavanagh, Christine O'Connor and Darren M. Griffith

\*

### **Supporting Information**

### [Ga(bipy)<sub>2</sub>(2,3-DHBA<sub>2H</sub>)](NO<sub>3</sub>).H<sub>2</sub>O (1)

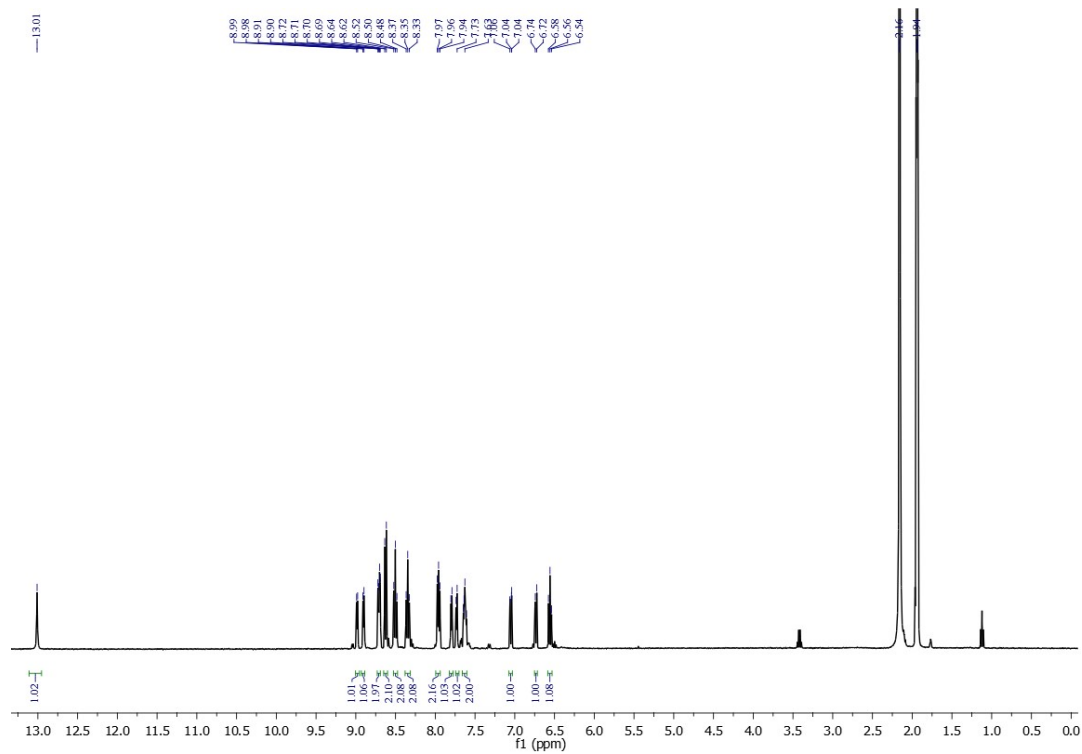


Figure S1.  $^1\text{H}$  NMR spectrum of **1** (in  $\text{CD}_3\text{CN}$ ).

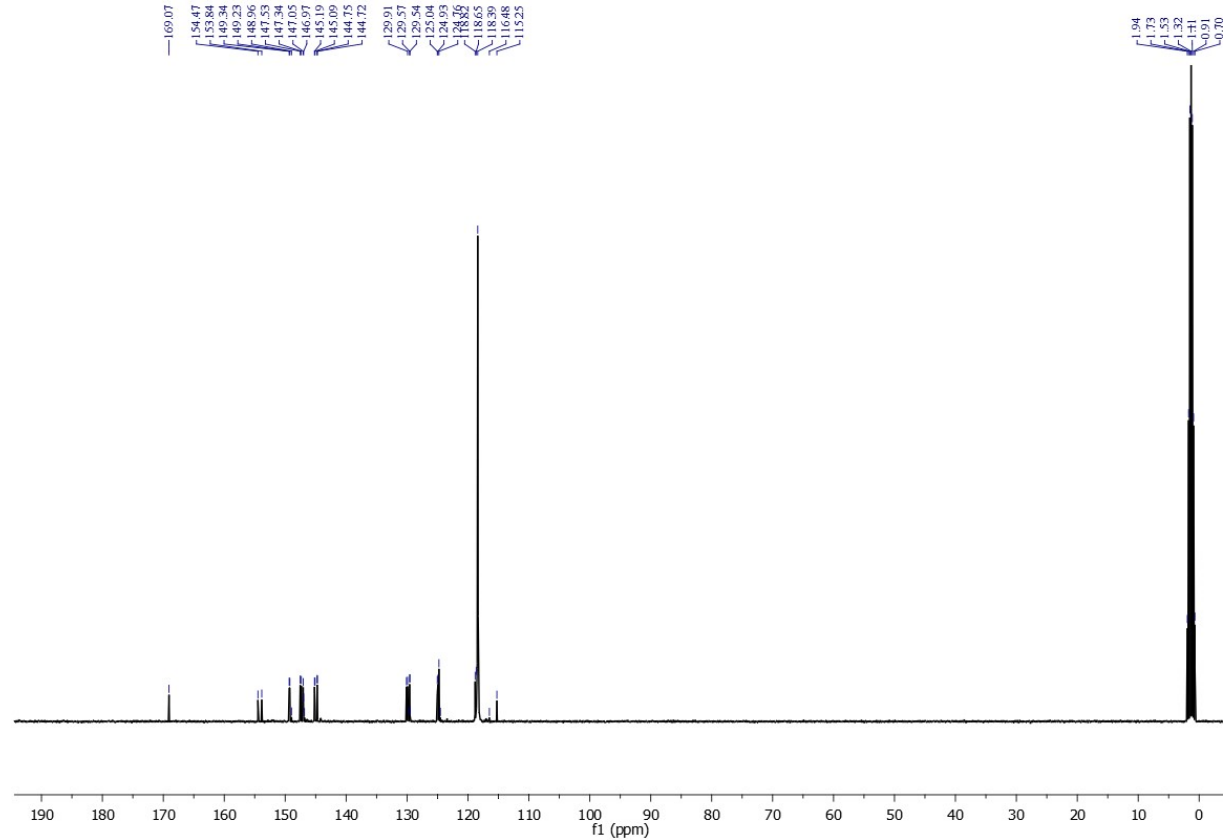


Figure S2.  $^{13}\text{C}$  NMR spectrum of **1** (in  $\text{CD}_3\text{CN}$ ).

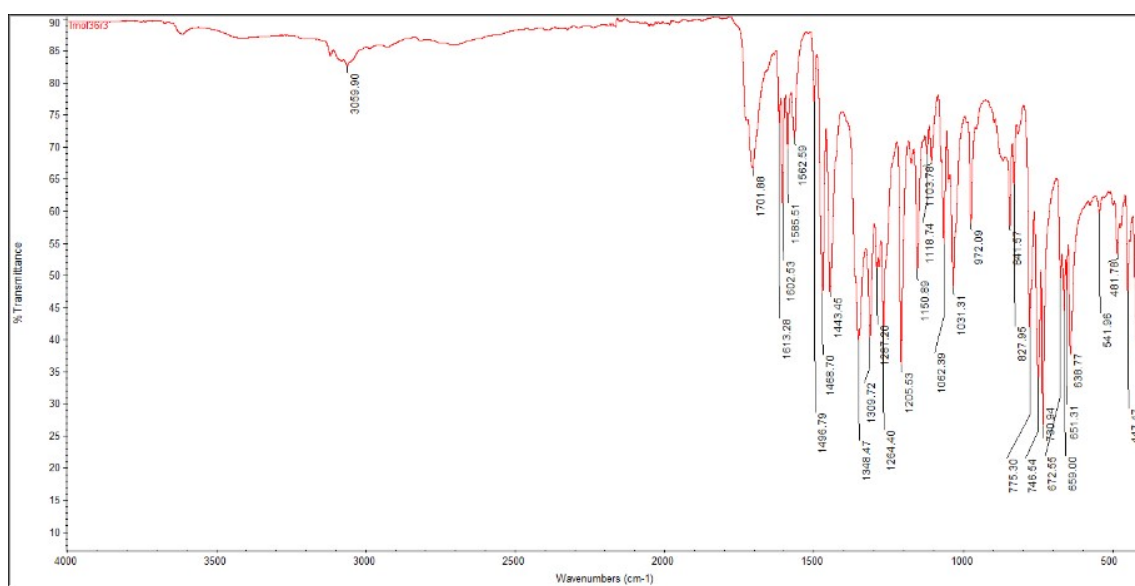


Figure S3. IR spectrum of **1**.

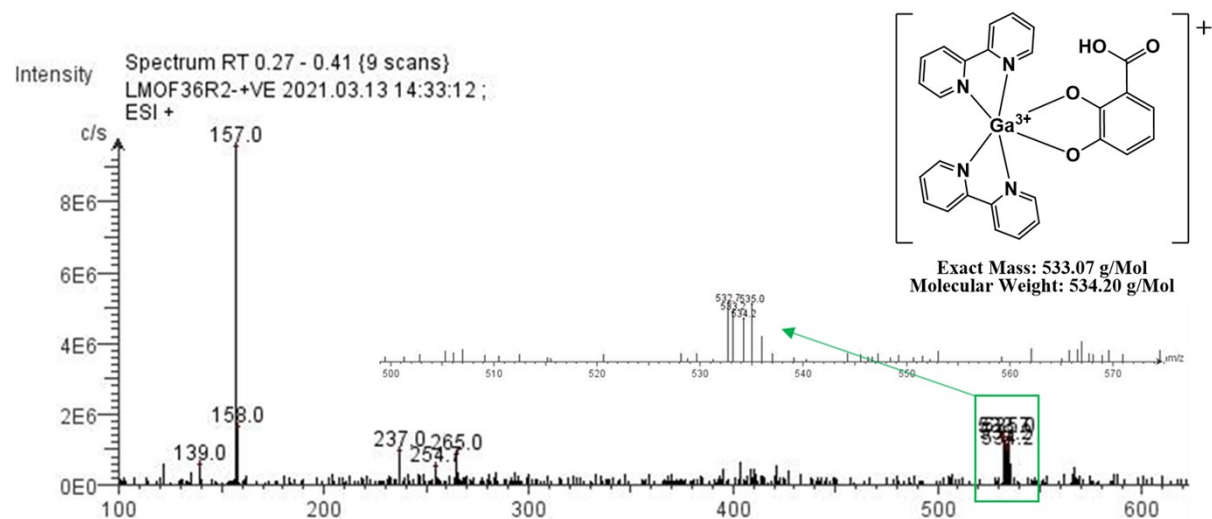


Figure S4. ESI mass spectrum of **1** (positive mode).

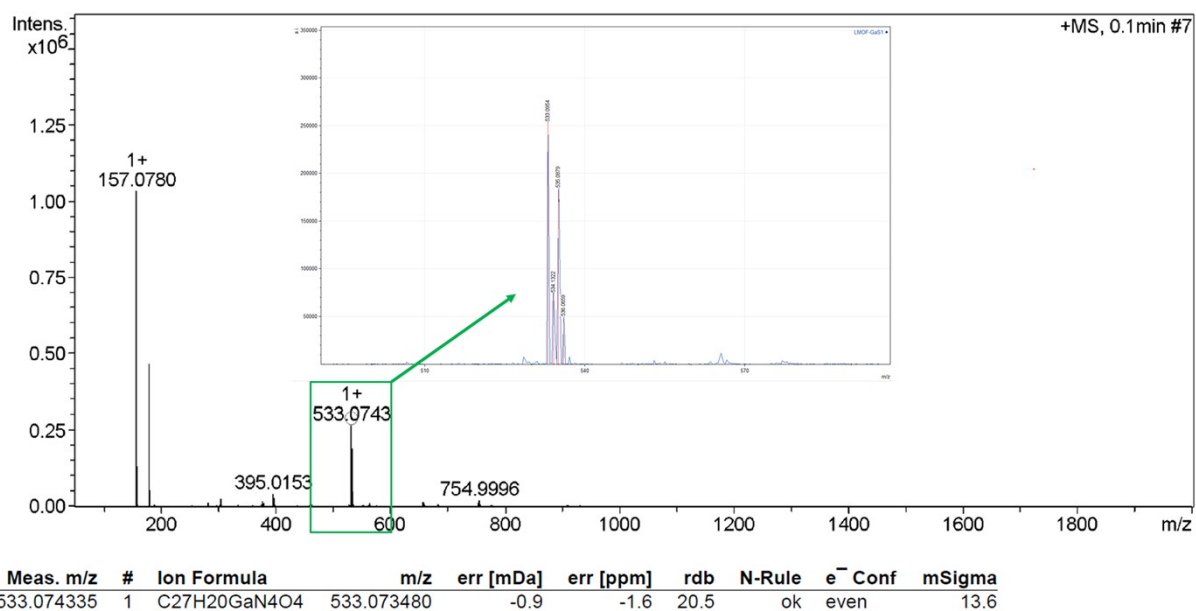


Figure S5. HR-MS ESI mass spectrum of **1** (positive mode).

**[Ga(bipy)<sub>2</sub>(3,4-DHBA-<sub>2</sub>H)](NO<sub>3</sub>).H<sub>2</sub>O (2)**

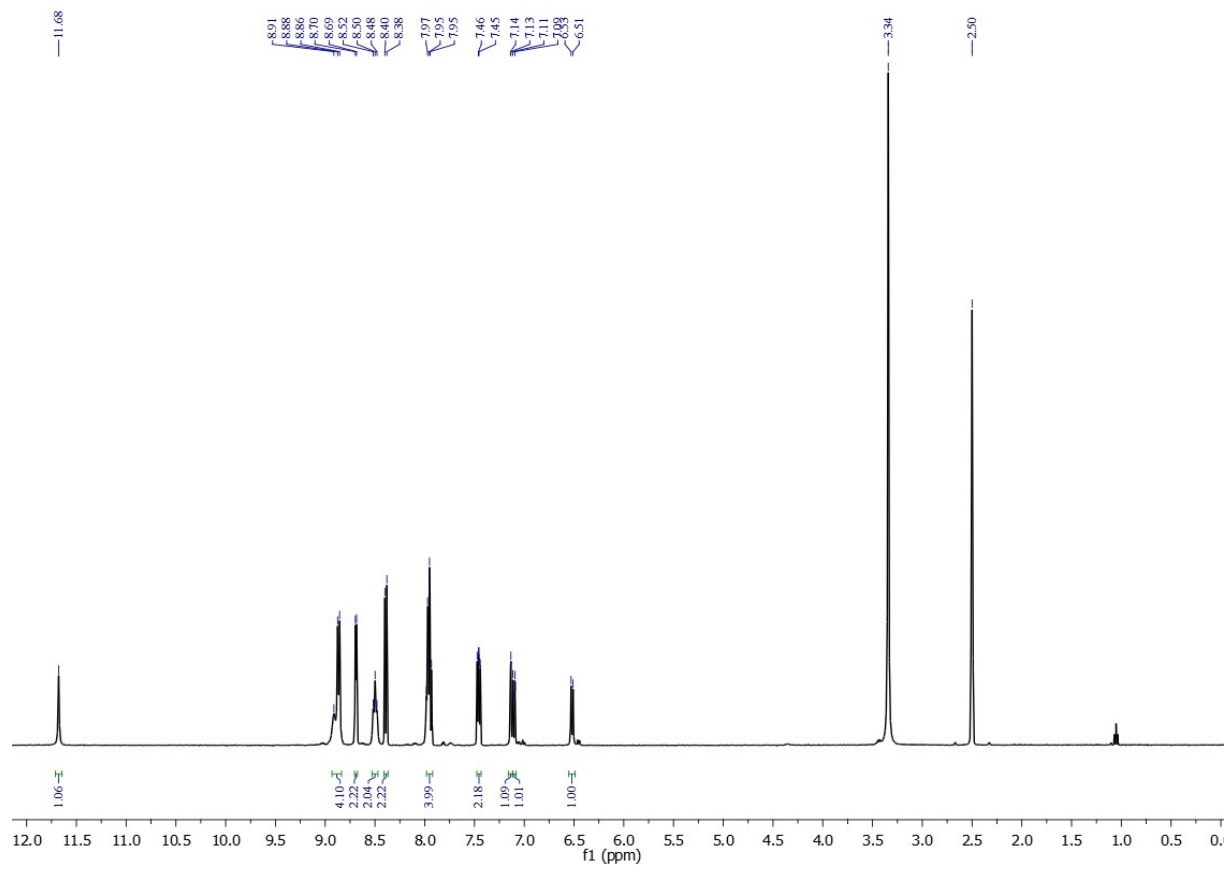


Figure S6. <sup>1</sup>H NMR spectrum of **2** (in DMSO-*d*<sup>6</sup>).

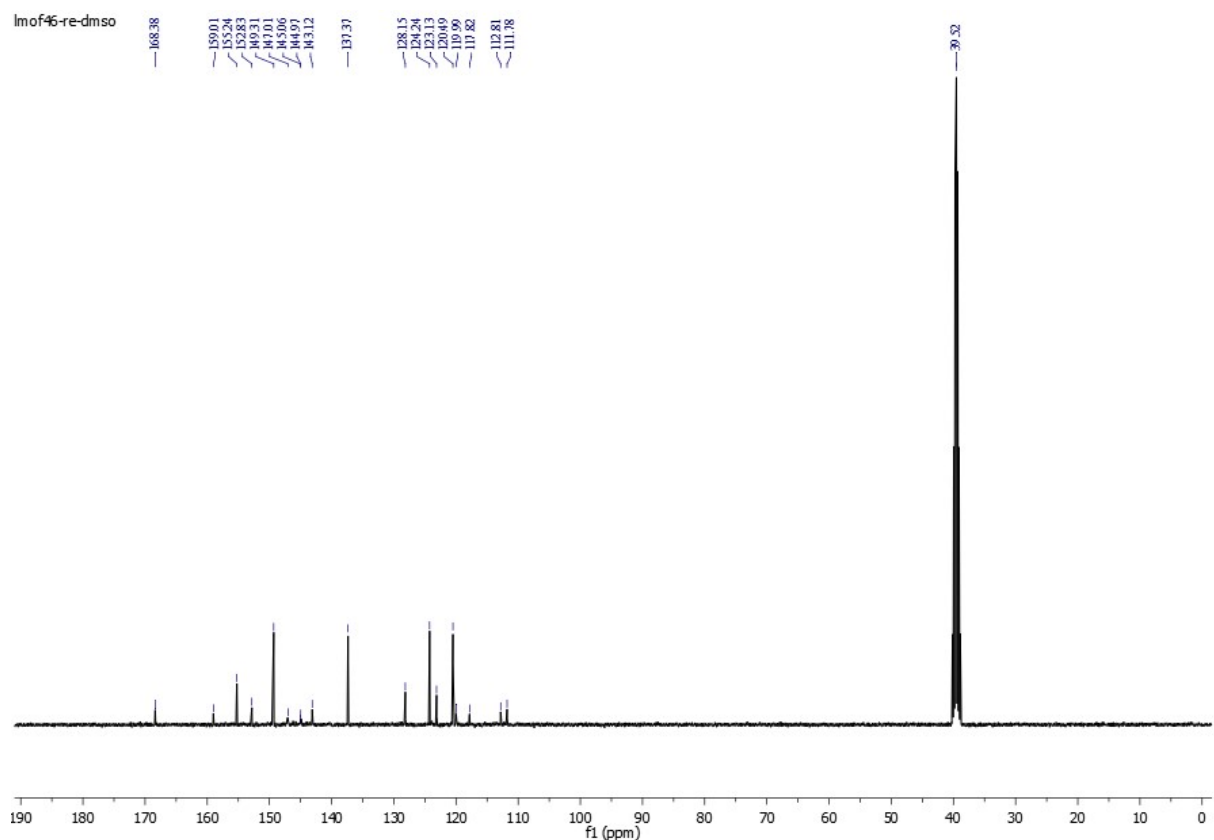


Figure S7.  $^{13}\text{C}$  NMR spectrum of **2** (in  $\text{DMSO}-d^6$ ).

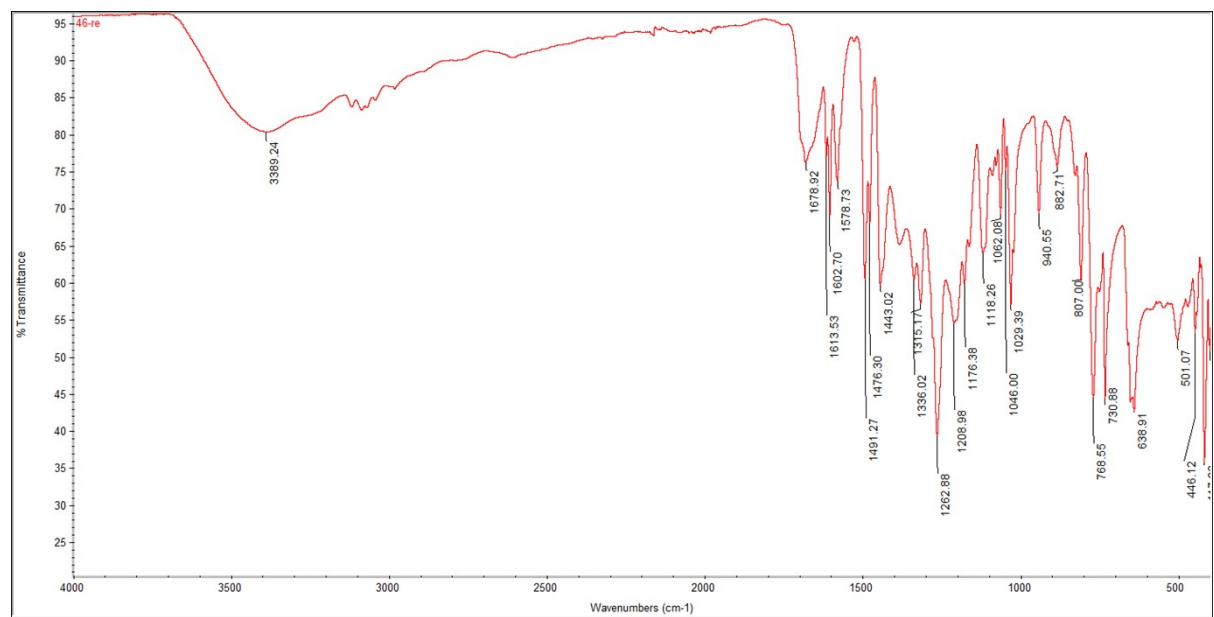


Figure S8. IR spectrum of **2**.

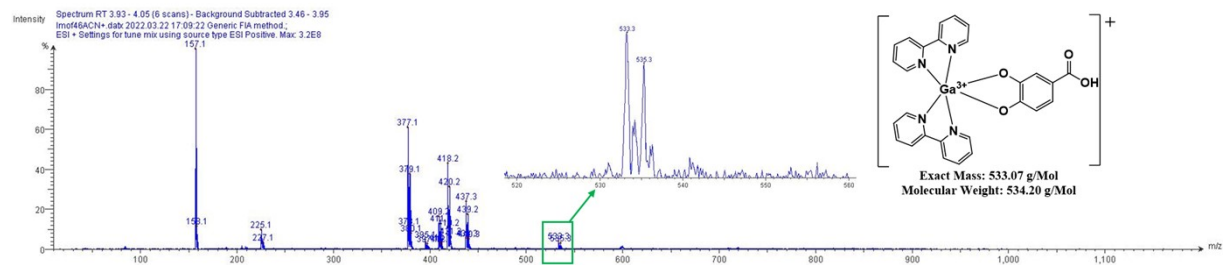


Figure S9. ESI mass spectrum of **2** (in positive mode).

**[Ga(bipy)<sub>2</sub>(3,4,5-THBA-<sub>2</sub>H)](NO<sub>3</sub>).H<sub>2</sub>O (3)**

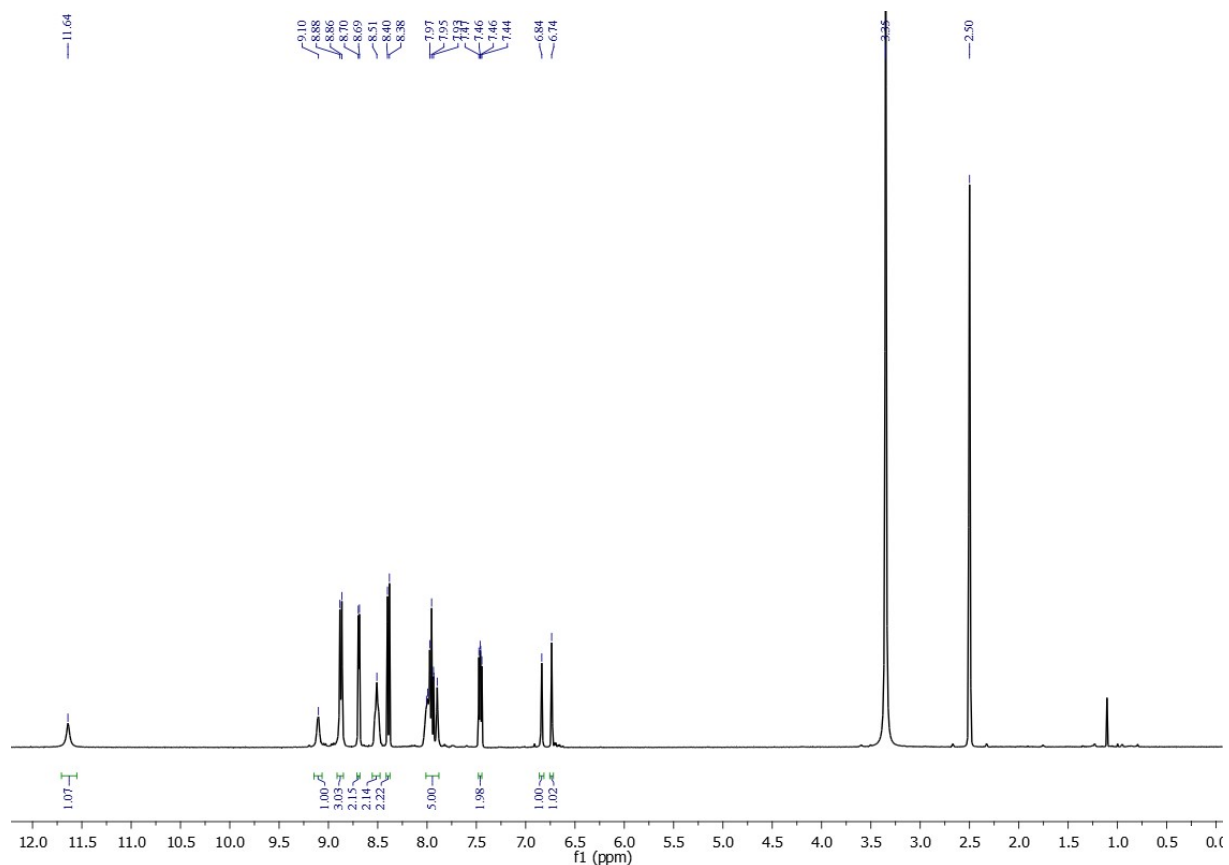


Figure S10. <sup>1</sup>H Figure S5. <sup>13</sup>H NMR spectrum of **3** (in DMSO-*d*<sup>6</sup>).

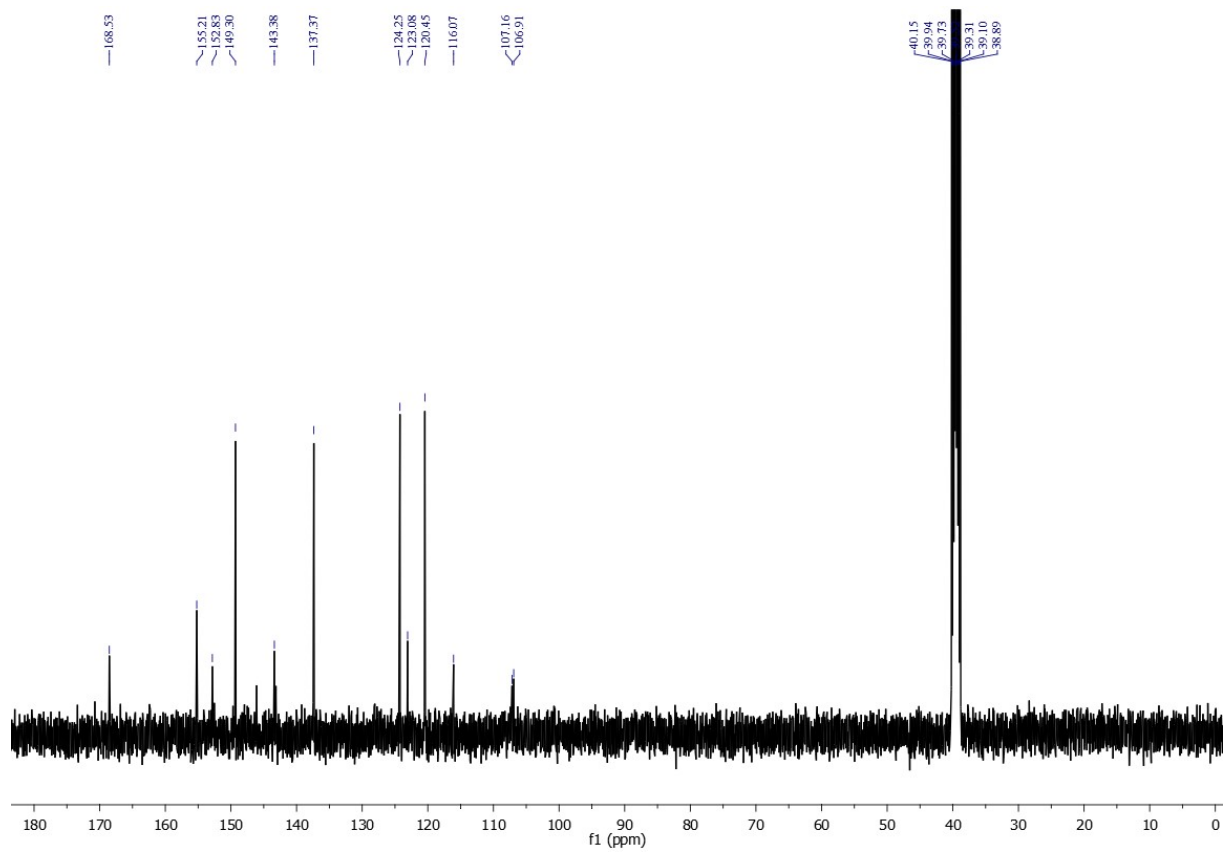


Figure S11.  $^{13}\text{C}$  NMR spectrum of **3** (in  $\text{DMSO}-d^6$ ).

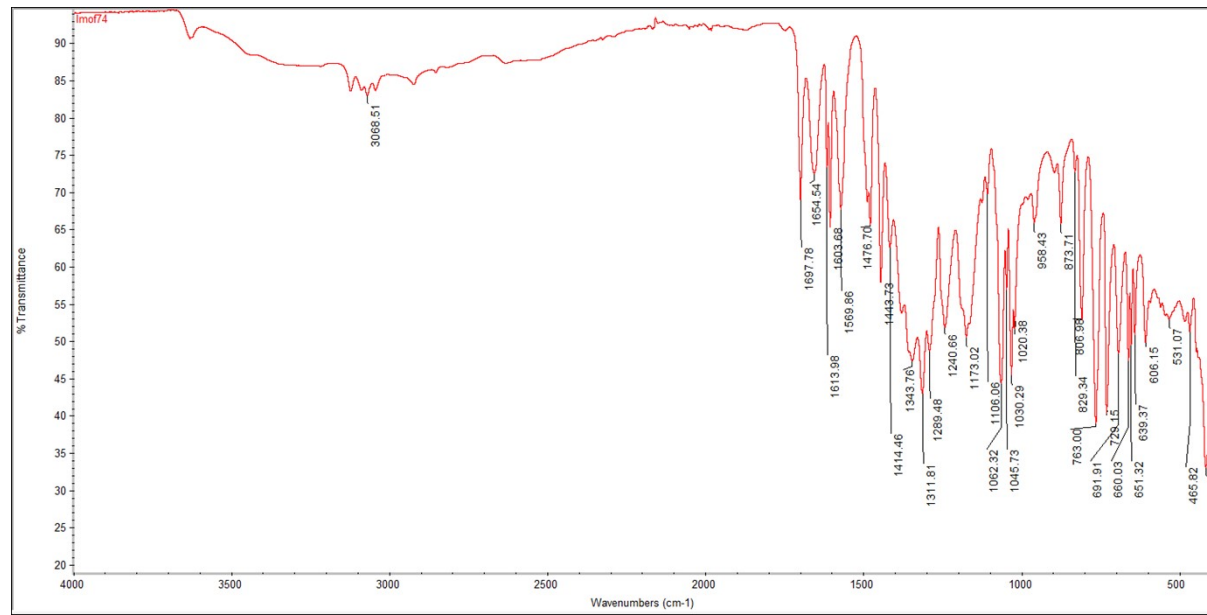


Figure S12. IR spectrum of **3**.

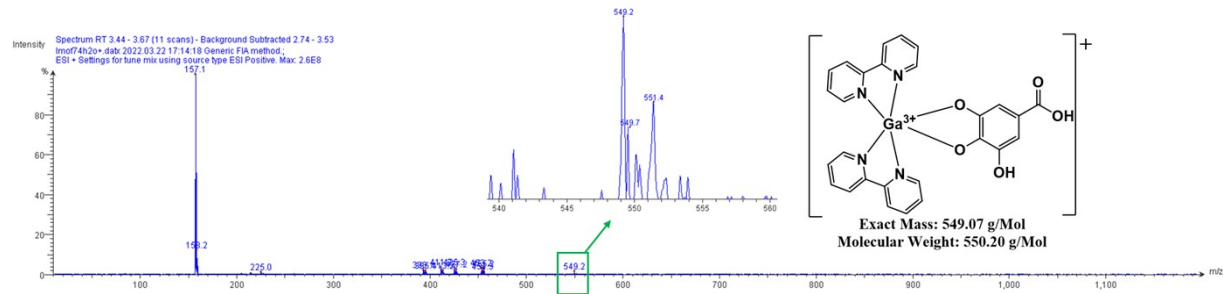


Figure S13. ESI mass spectrum of **3** (in positive mode).

**[Ga(phen)<sub>2</sub>(2,3DHBA-<sub>2</sub>H)](NO<sub>3</sub>).H<sub>2</sub>O (4)**

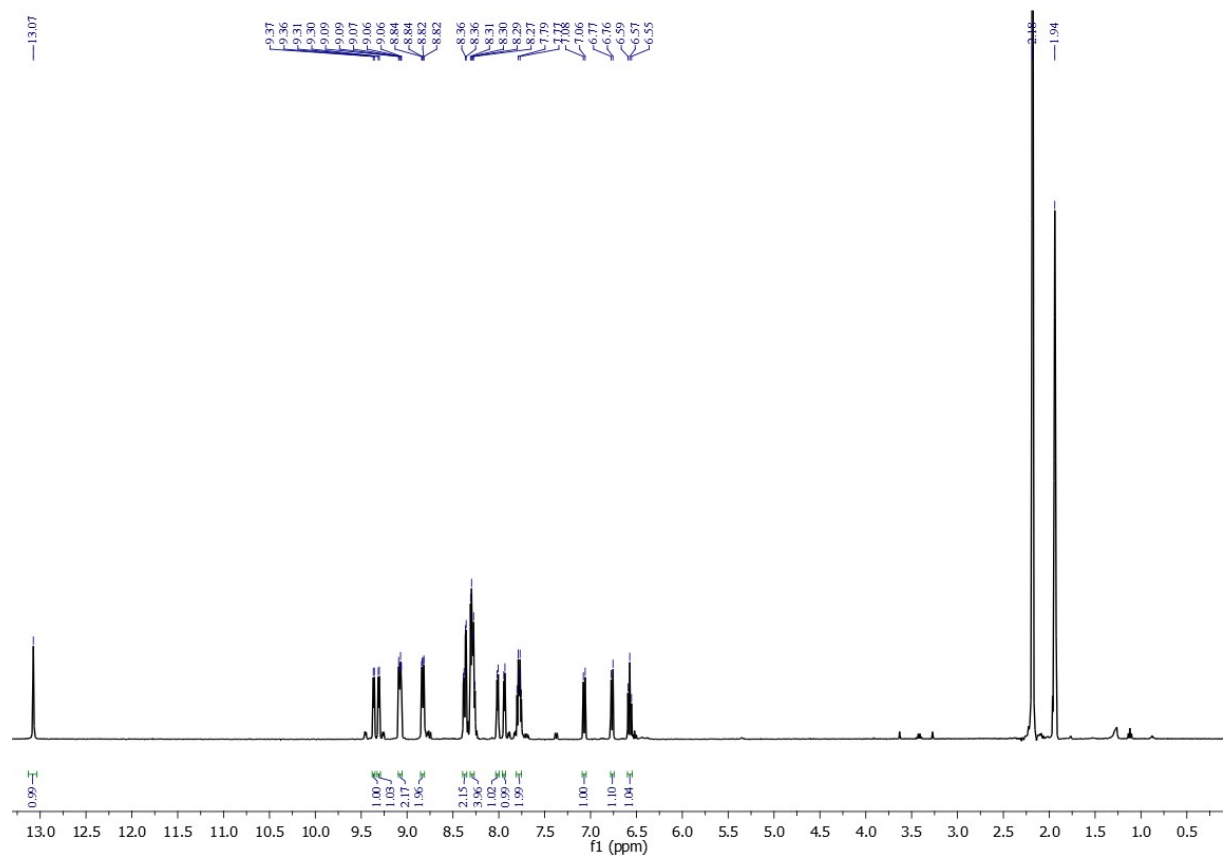


Figure S14. <sup>1</sup>H NMR spectrum of **4** (in CD<sub>3</sub>CN).

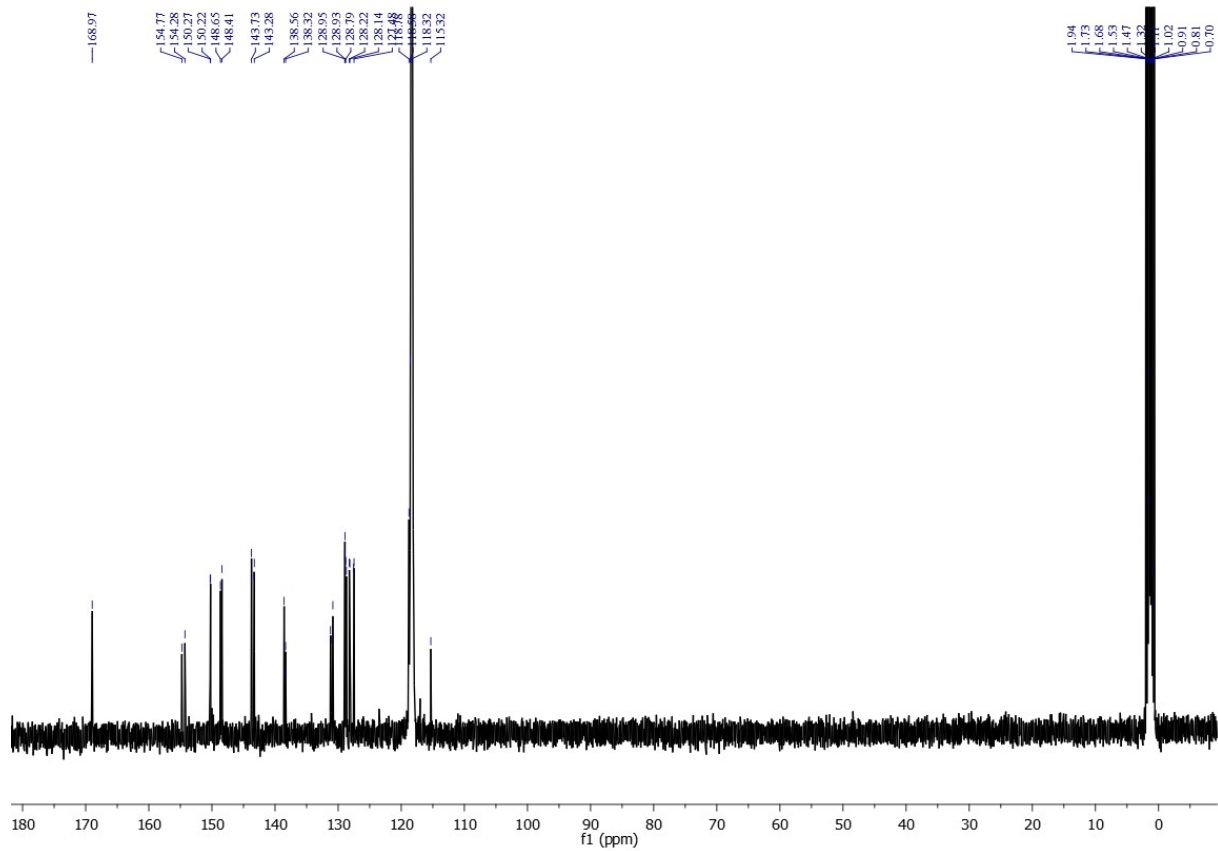


Figure S15.  $^{13}\text{C}$  NMR spectrum of **4** (in  $\text{CD}_3\text{CN}$ ).

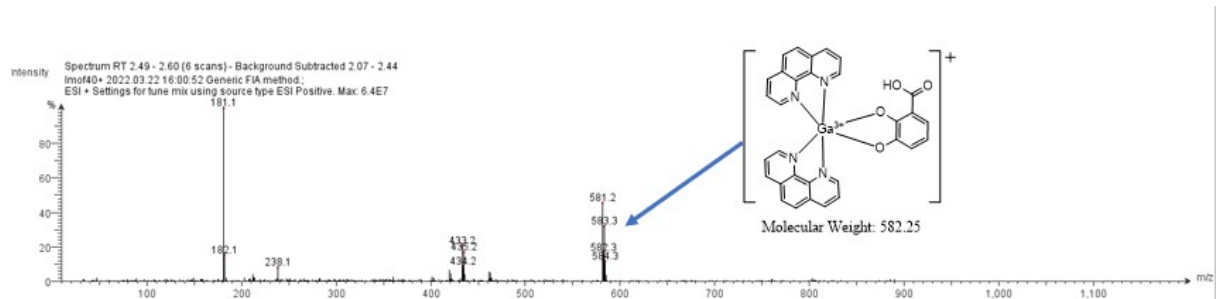


Figure S16. ESI mass spectrum of **4** (in positive mode).

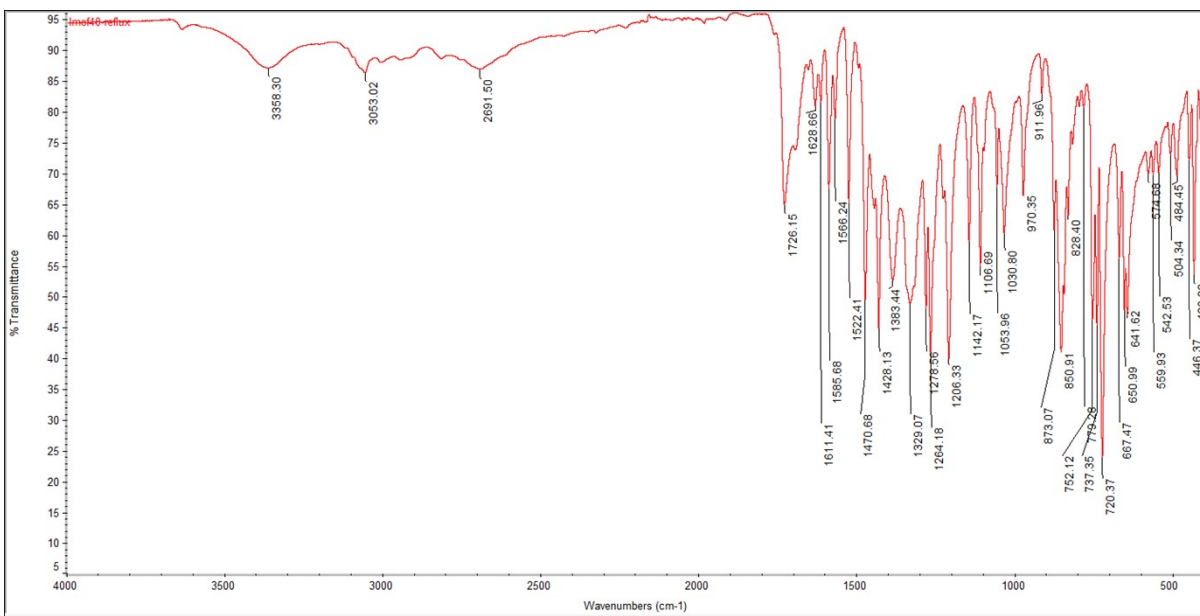


Figure S17. IR spectrum of **4**.

### [Ga(bipy)<sub>2</sub>(CafA-<sub>2</sub>H)](NO<sub>3</sub>).H<sub>2</sub>O (**5**)

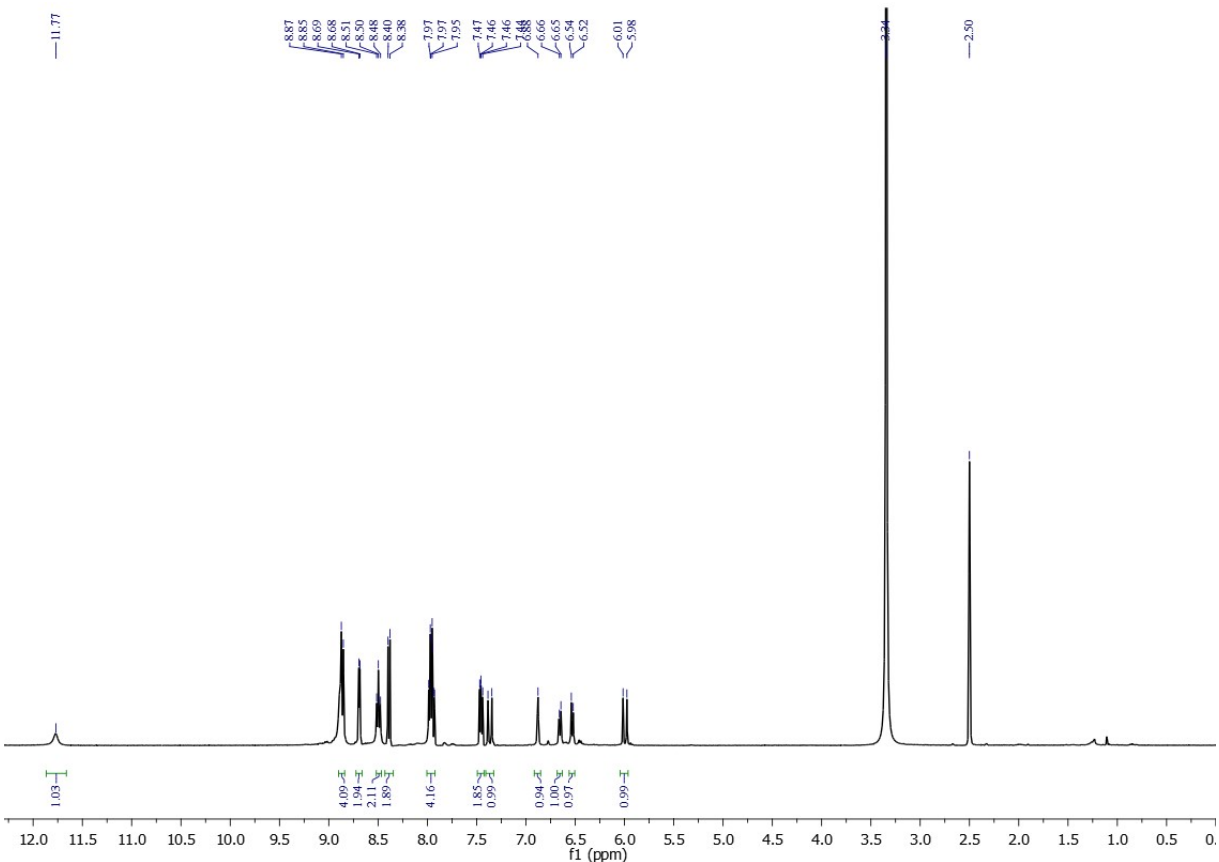


Figure S18. <sup>1</sup>H NMR spectrum of **5** (in DMSO-*d*<sup>6</sup>).

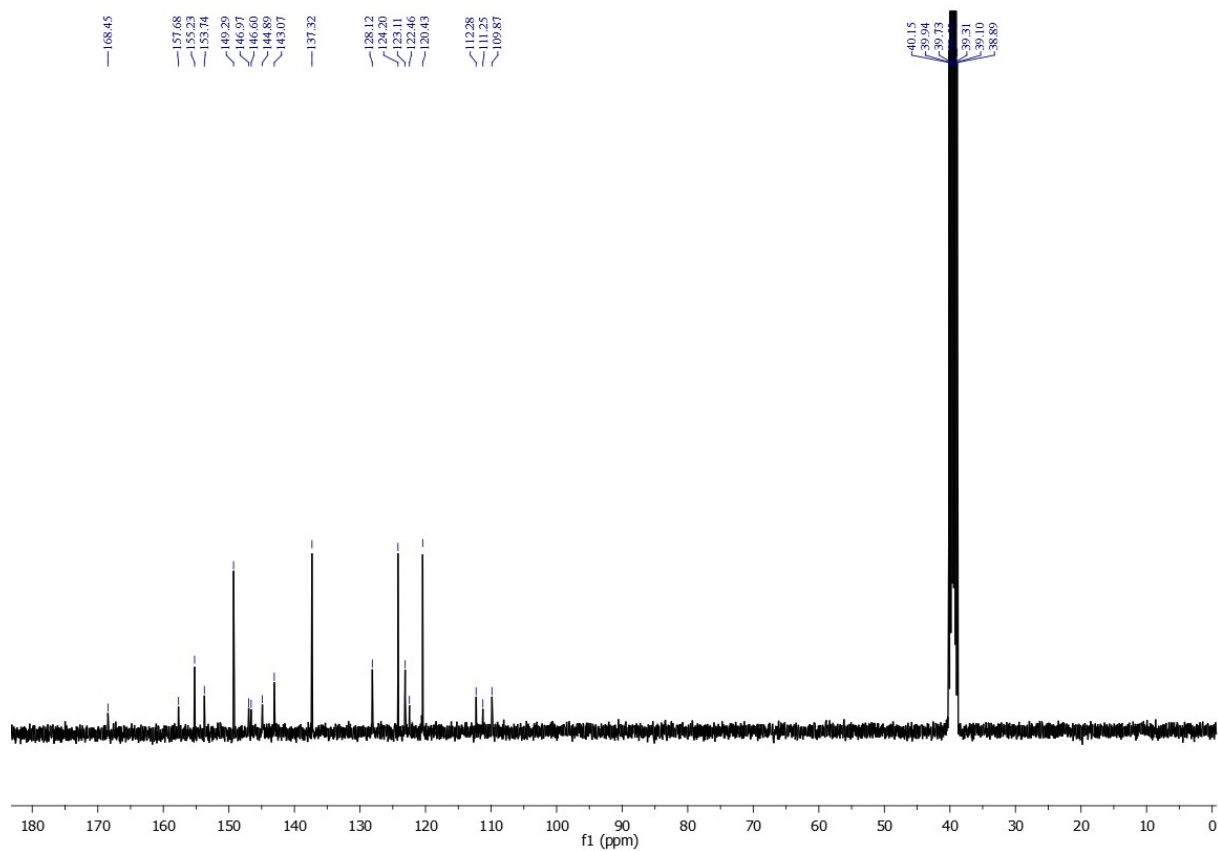


Figure S19.  $^{13}\text{C}$  NMR spectrum of **5** (in  $\text{DMSO}-d^6$ ).

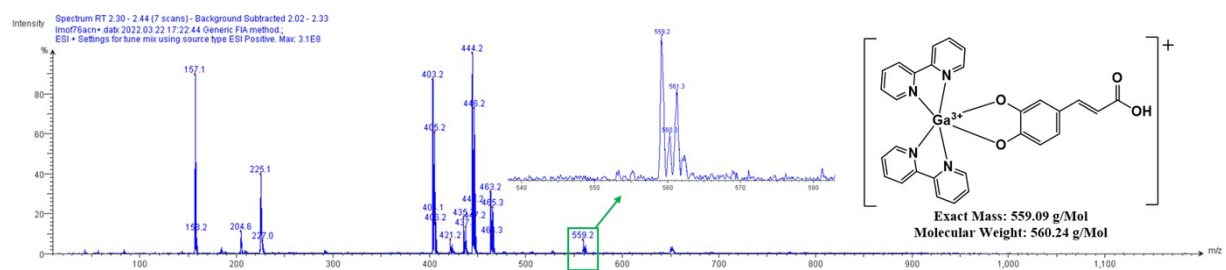


Figure S20. ESI mass spectrum of **5** (in positive mode).

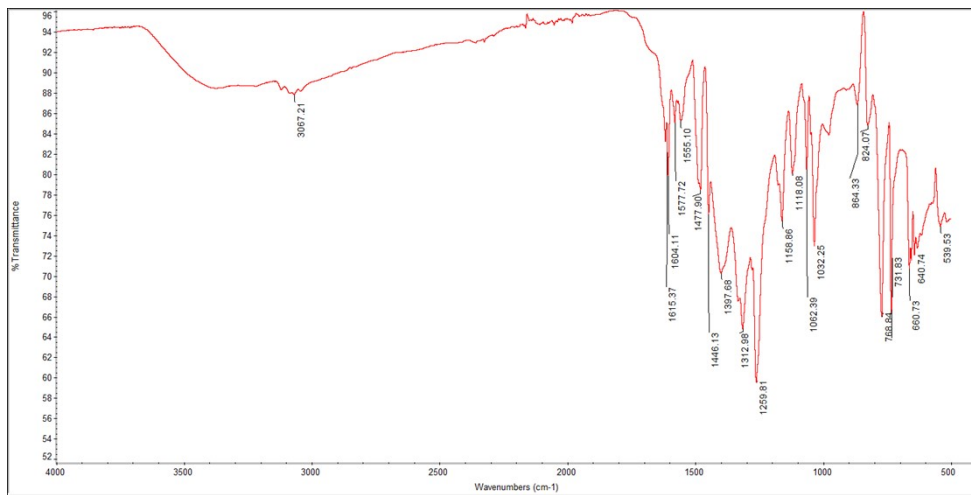


Figure S21. IR spectrum of **5**.

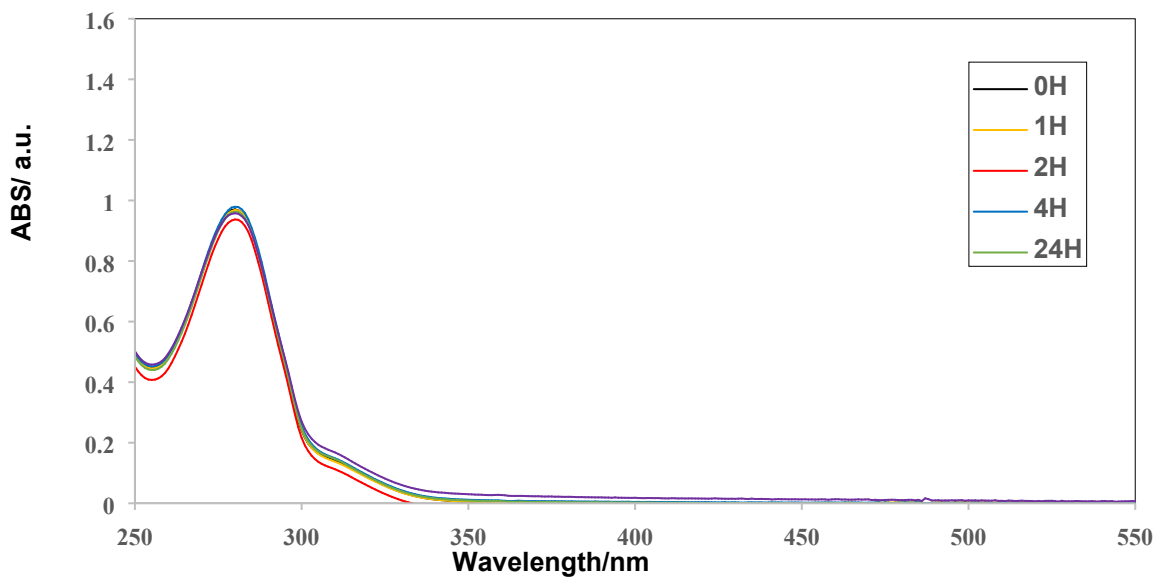


Figure S22. UV-Vis spectrum of **1** (50  $\mu\text{M}$ ) in water over the course of 24 h at 37°C.

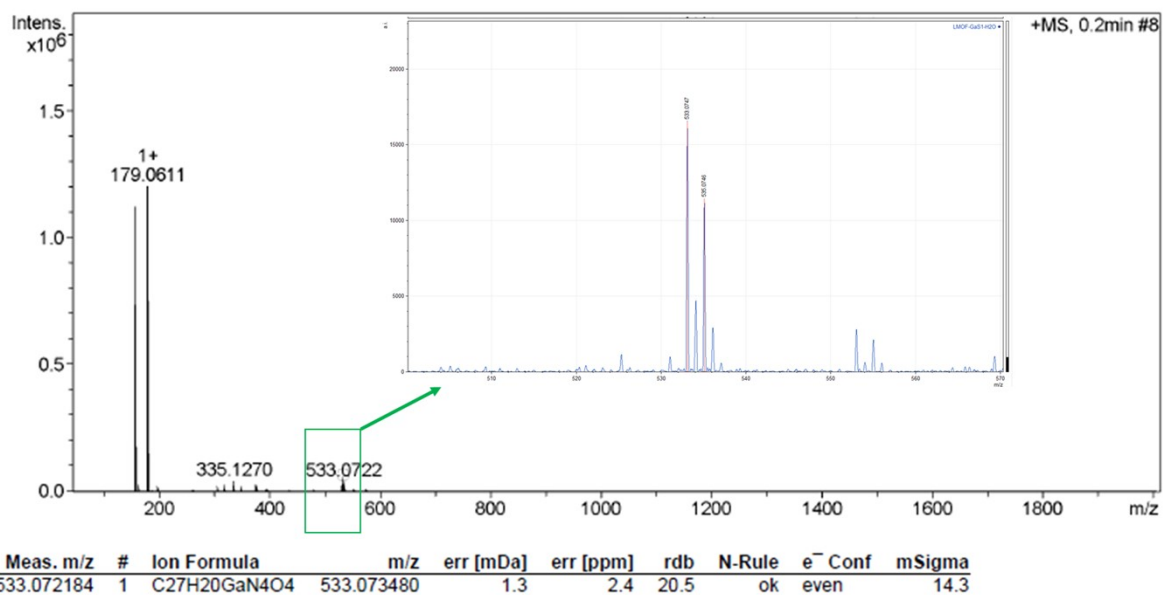


Figure S23. HRMS spectrum of **1** after 24 h in water at 37°C.

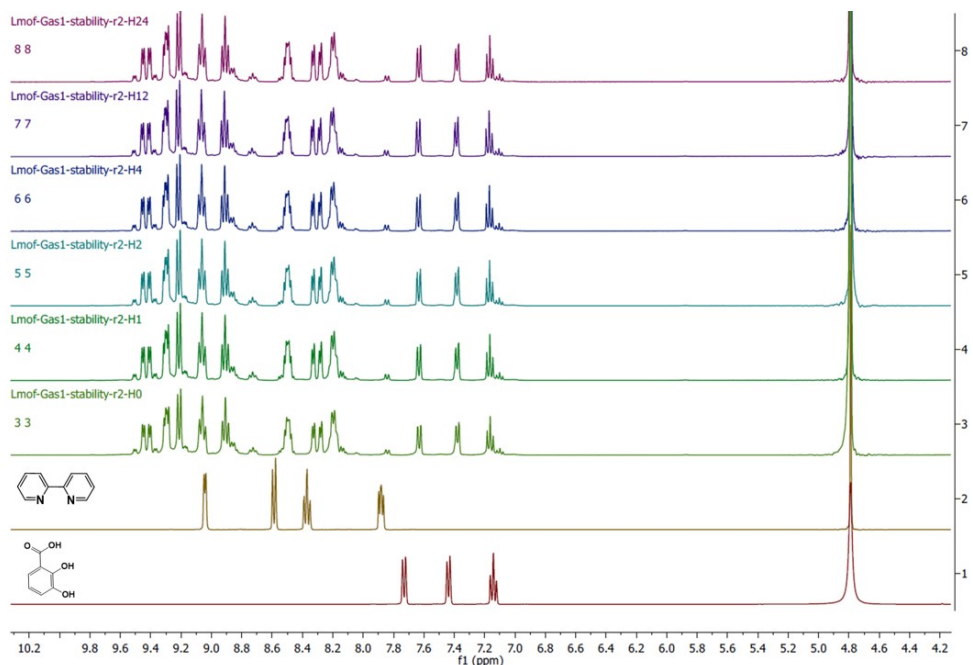


Figure S24. <sup>1</sup>H NMR study of **1** in D<sub>2</sub>O:CD<sub>3</sub>CN (50:50) over 24 h at 37 °C stacked with <sup>1</sup>H NMR spectra of bipy and 2,3-DHBA in D<sub>2</sub>O:CD<sub>3</sub>CN (50:50).

Table S1. Crystal data and structure refinement for **1** to **4**.

Identification code	<b>1</b>	<b>2</b>	<b>3</b>	<b>4</b>
Empirical formula	C <sub>28</sub> H <sub>24</sub> F <sub>6</sub> GaN <sub>4</sub> O <sub>5</sub> P	C <sub>27</sub> H <sub>20</sub> F <sub>6</sub> GaN <sub>4</sub> O <sub>4</sub> P	C <sub>27.2</sub> H <sub>24.97</sub> Cl <sub>0.5</sub> F <sub>3</sub> GaN <sub>4</sub> O <sub>7.28</sub> P <sub>0.5</sub>	C <sub>32.5</sub> H <sub>24.5</sub> F <sub>6</sub> GaN <sub>4</sub> O <sub>4.75</sub> P
Formula weight	711.20	679.16	684.34	761.75
Temperature/K	100(2)	100(2)	100(2)	100(2)
Crystal system	monoclinic	monoclinic	tetragonal	monoclinic
Space group	C2/c	P2 <sub>1</sub> /c	I4 <sub>1</sub> /acd	P2 <sub>1</sub> /c
a (Å)	24.412(2)	24.4395(7)	32.0378(10)	15.8706(9)
b (Å)	9.5067(8)	8.6262(3)	32.0378(10)	8.8591(5)
c (Å)	23.7787(19)	26.9096(7)	23.4142(11)	23.0866(12)
α (°)	90	90	90	90
β (°)	93.720(2)	110.5153(14)	90	109.0030(10)
γ (°)	90	90	90	90
Volume (Å <sup>3</sup> )	5506.9(8)	5313.3(3)	24032.8(19)	3069.1(3)
Z	8	8	32	4
ρ <sub>calc</sub> (g/cm <sup>3</sup> )	1.716	1.698	1.513	1.649
μ (mm <sup>-1</sup> )	1.147	2.771	1.057	1.035
F(000)	2880.0	2736.0	11150.0	1542.0
Crystal size (mm <sup>3</sup> )	0.34 × 0.09 × 0.05	0.226 × 0.136 × 0.032	0.197 × 0.168 × 0.13	0.284 × 0.117 × 0.072
Radiation	Mo Kα (λ = 0.71073)	Cu Kα (λ = 1.54178)	Mo Kα (λ = 0.71073)	Mo Kα (λ = 0.71073)
Reflections collected	30714	103969	109222	47191
Independent reflections	5725 R <sub>int</sub> = 0.1300, R <sub>sigma</sub> = 0.0839	10065 R <sub>int</sub> = 0.0716, R <sub>sigma</sub> = 0.0358	5574 R <sub>int</sub> = 0.1062, R <sub>sigma</sub> = 0.0300	7116 R <sub>int</sub> = 0.0873, R <sub>sigma</sub> = 0.0472
Data/restraints/parameters	5725/2/414	10065/1185/1 057	5574/82/464	7116/228/535
Goodness-of-fit on F <sup>2</sup>	1.015	1.056	1.073	1.068
Final R indexes [I≥2σ (I)]*	R <sub>1</sub> = 0.0319, wR <sub>2</sub> = 0.0824	R <sub>1</sub> = 0.0436, wR <sub>2</sub> = 0.0996	R <sub>1</sub> = 0.0339, wR <sub>2</sub> = 0.0829	R <sub>1</sub> = 0.0581, wR <sub>2</sub> = 0.1330
Final R indexes [all data]	R <sub>1</sub> = 0.0381, wR <sub>2</sub> = 0.0872	R <sub>1</sub> = 0.0672, wR <sub>2</sub> = 0.1127	R <sub>1</sub> = 0.0391, wR <sub>2</sub> = 0.0868	R <sub>1</sub> = 0.0876, wR <sub>2</sub> = 0.1465
Largest diff. peak/hole (e Å <sup>-3</sup> )	0.33/-0.19	0.44/-0.27	0.34/-0.24	1.13/-1.10

$$*R_1 = \sum ||F_o| - |F_c|| / \sum |F_o|, wR_2 = [\sum w(F_o^2 - F_c^2)^2 / \sum w(F_o^2)^2]^{1/2}.$$

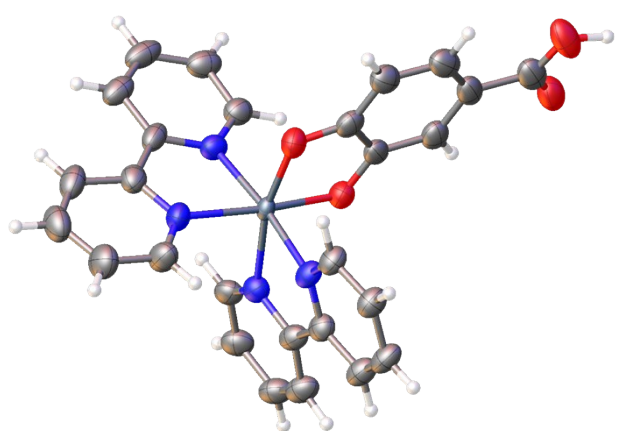


Fig. S25. Major occupied moiety (65% occupied) of one of the two independent cations in the asymmetric unit of **2** with displacement shown at 50% probability. See SI Fig S23 for the complete asymmetric unit of the  $\text{PF}_6^-$  salt.

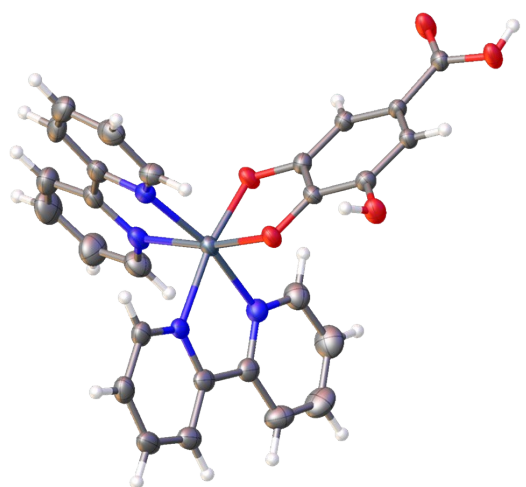


Fig. S26. Structure of the complex cation of **3** only with displacement shown at 50% probability. The salt is comprised of a mixed  $\text{PF}_6^-/\text{Cl}^-$  anion with  $\text{H}_2\text{O}$  and  $\text{MeOH}$  solvates which are not shown. See SI Fig S24 for the complete asymmetric unit of the mixed anion salt.

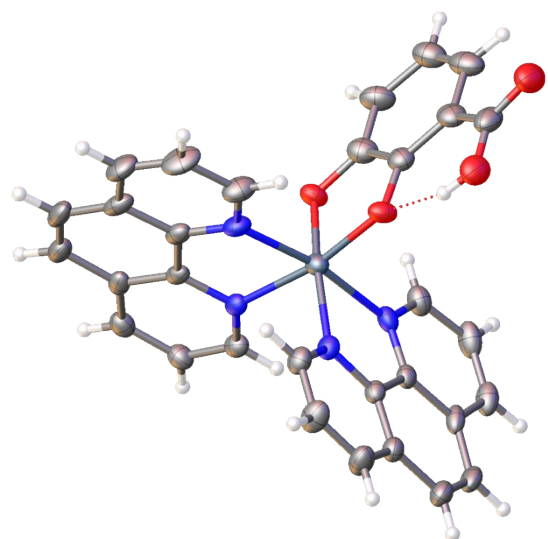


Fig. S27. Structure of complex cation of **4** with displacement shown at 50% probability. A  $\text{PF}_6^-$  salt, solvated with partially occupied EtOH are not shown. See SI Fig S31 for the complete asymmetric unit.

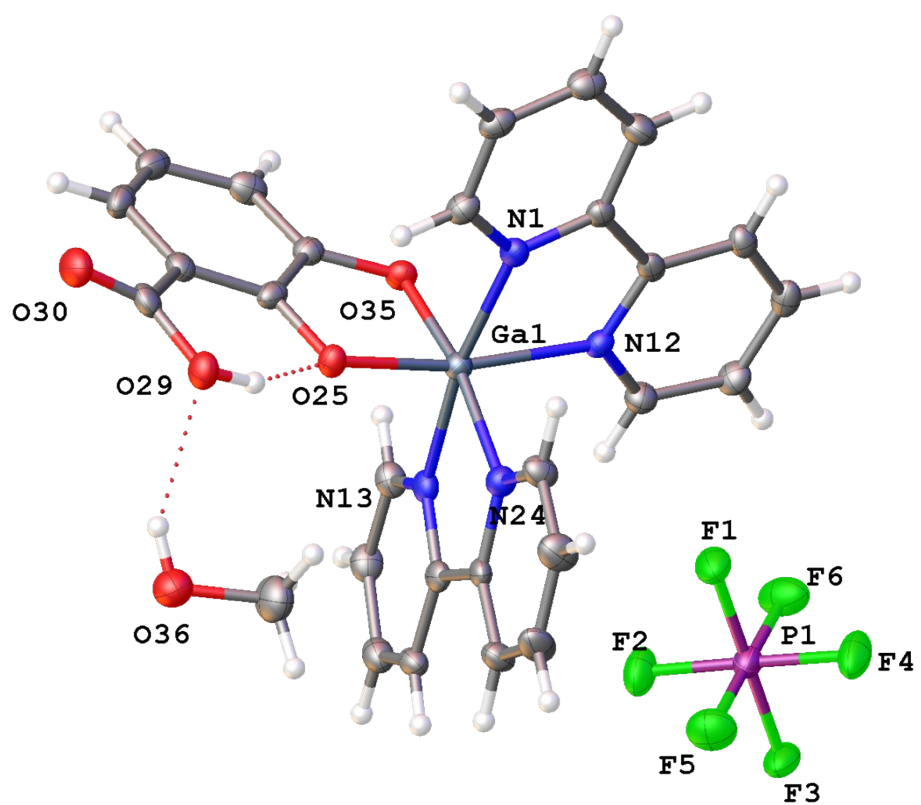
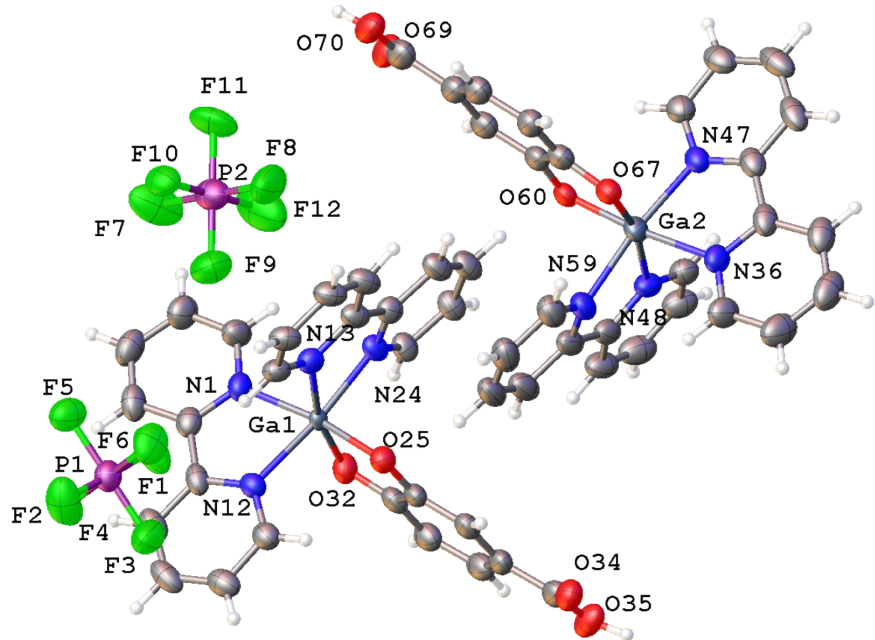
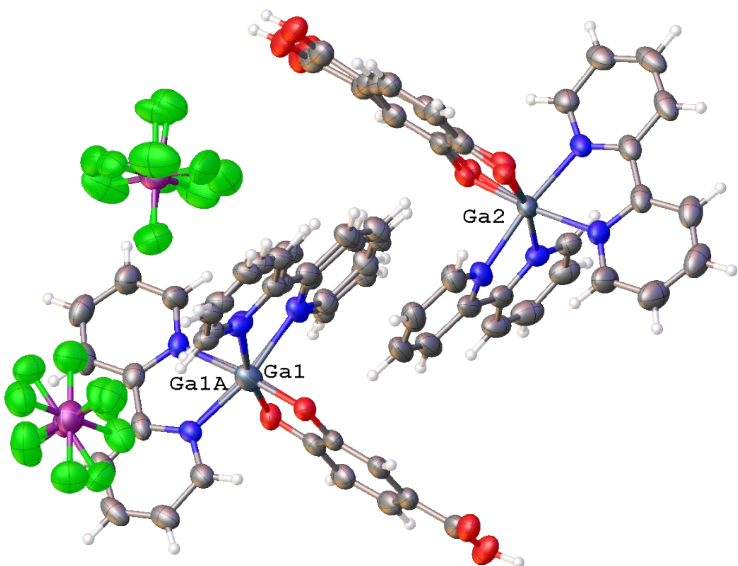


Fig. S28. Complete asymmetric unit of **1**, showing the  $\text{PF}_6^-$  anion and methanol solvate with heteroatoms labelled only. Displacement shown at 50% probability.



A



B

Fig. S29. Complete asymmetric unit of **2** with displacement shown at 50% probability showing (A) the majority occupied moiety only with Ga/bipy 65% and 3,4-DHBA 52%; PF<sub>6</sub>, P1: 83% and P2: 53% occupied with heteroatoms labelled only and (B) showing the complete disordered ion pairs.

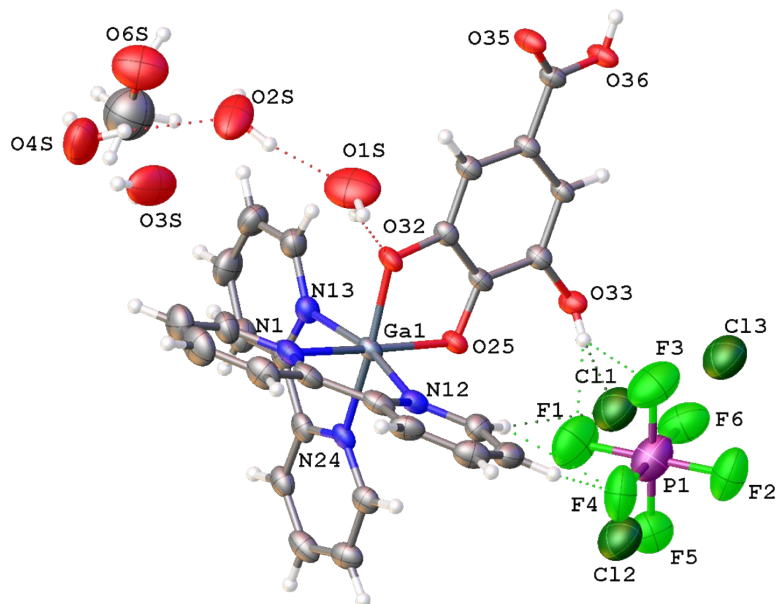


Fig. S30. **3** complete ion pair, showing the full asymmetric unit with mixed  $\text{PF}_6^-/\text{Cl}^-$  anion, water and methanol solvates.  $\text{PF}_6^-$  anion is 50% occupied and water solvent molecules modelled over 4 locations (100:50:33:25%) with a partially occupied MeOH (20%). The residual Cl anion occupies three sites. Atomic displacement shown at 50% probability and heteroatoms labelled only.

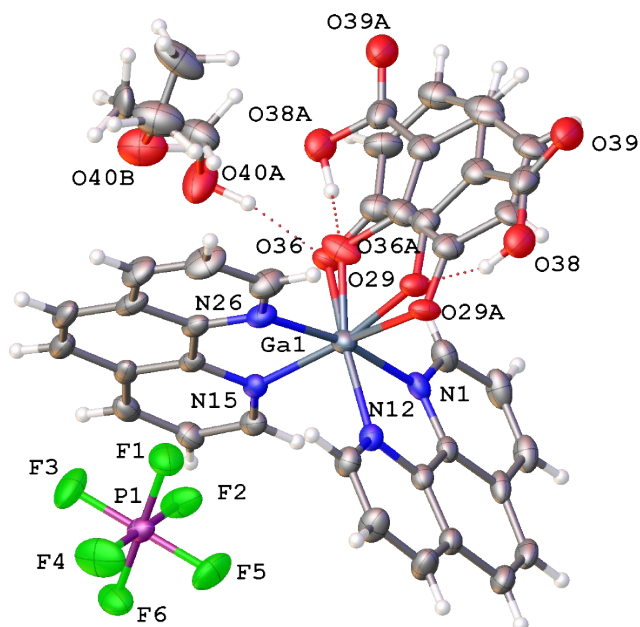


Fig. S31. Complete asymmetric unit of the ion pair in **4** showing the disorder in the 2,3-DHBA moiety (90:10% occupied). EtOH is 75% occupied over two locations (43:32%). Atomic displacement shown at 50% probability and heteroatoms labelled only.

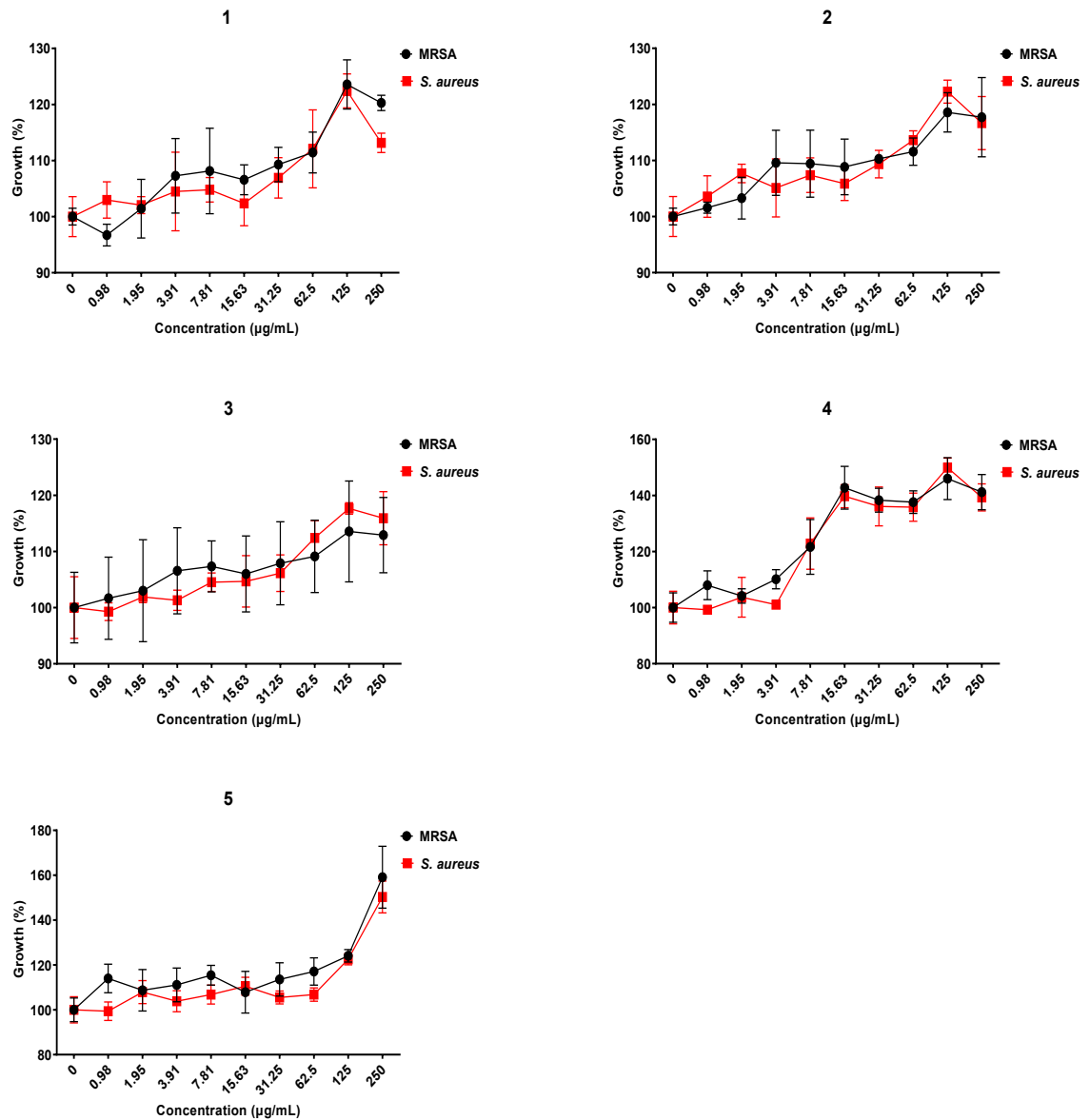


Figure S32. *in vitro* susceptibility assays for 1 to 5 against *S. aureus* and MRSA. GraphPad Prism, n= 3.

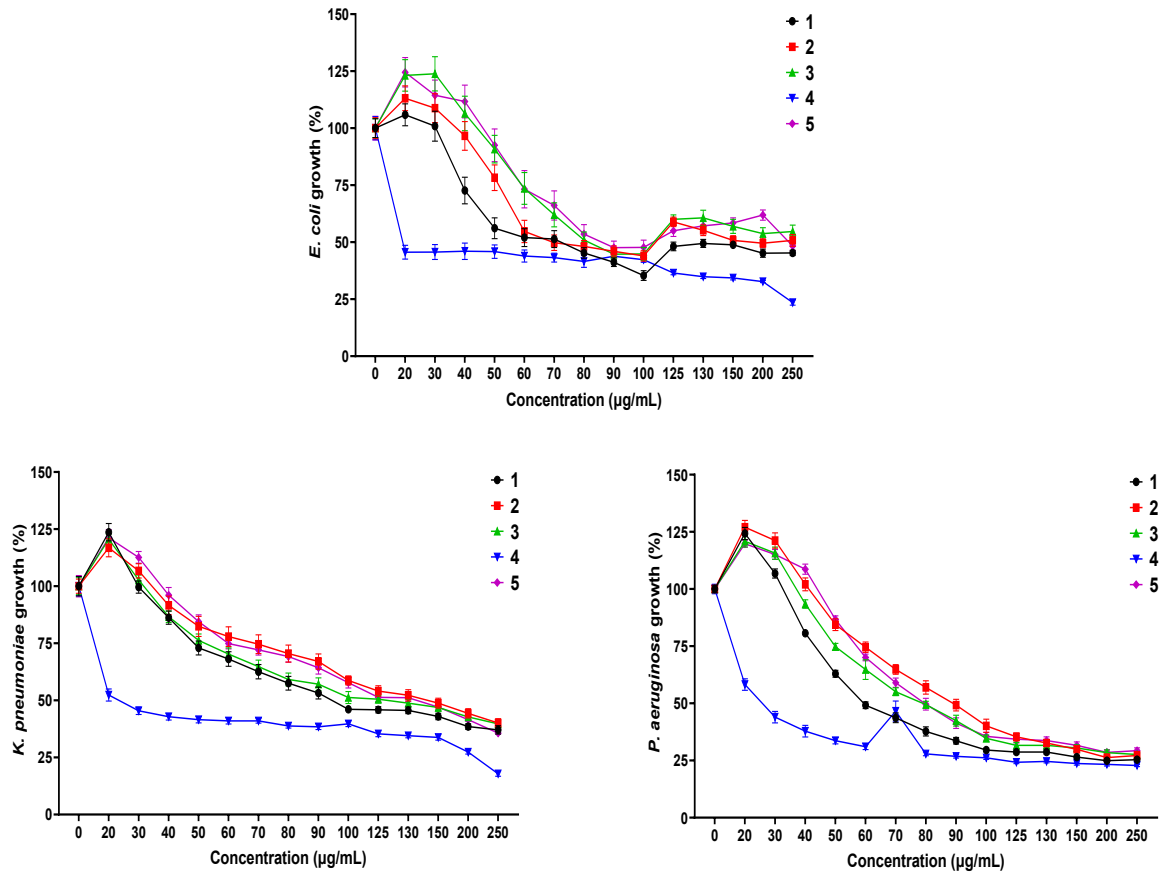


Figure S33. *in vitro* susceptibility assays for 1 to 5 against *E.coli*, *K. pneumoniae* and *P. aeruginosa*. GraphPad Prism, n= 3.

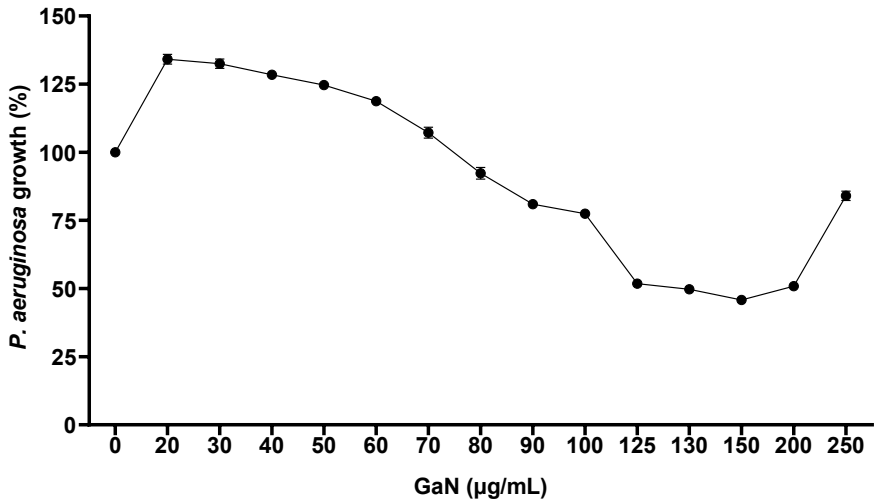


Figure S34. *in vitro* susceptibility assays for  $\text{GaN}$  against *E.coli*, *K. pneumoniae* and *P. aeruginosa*. GraphPad Prism, n= 3.

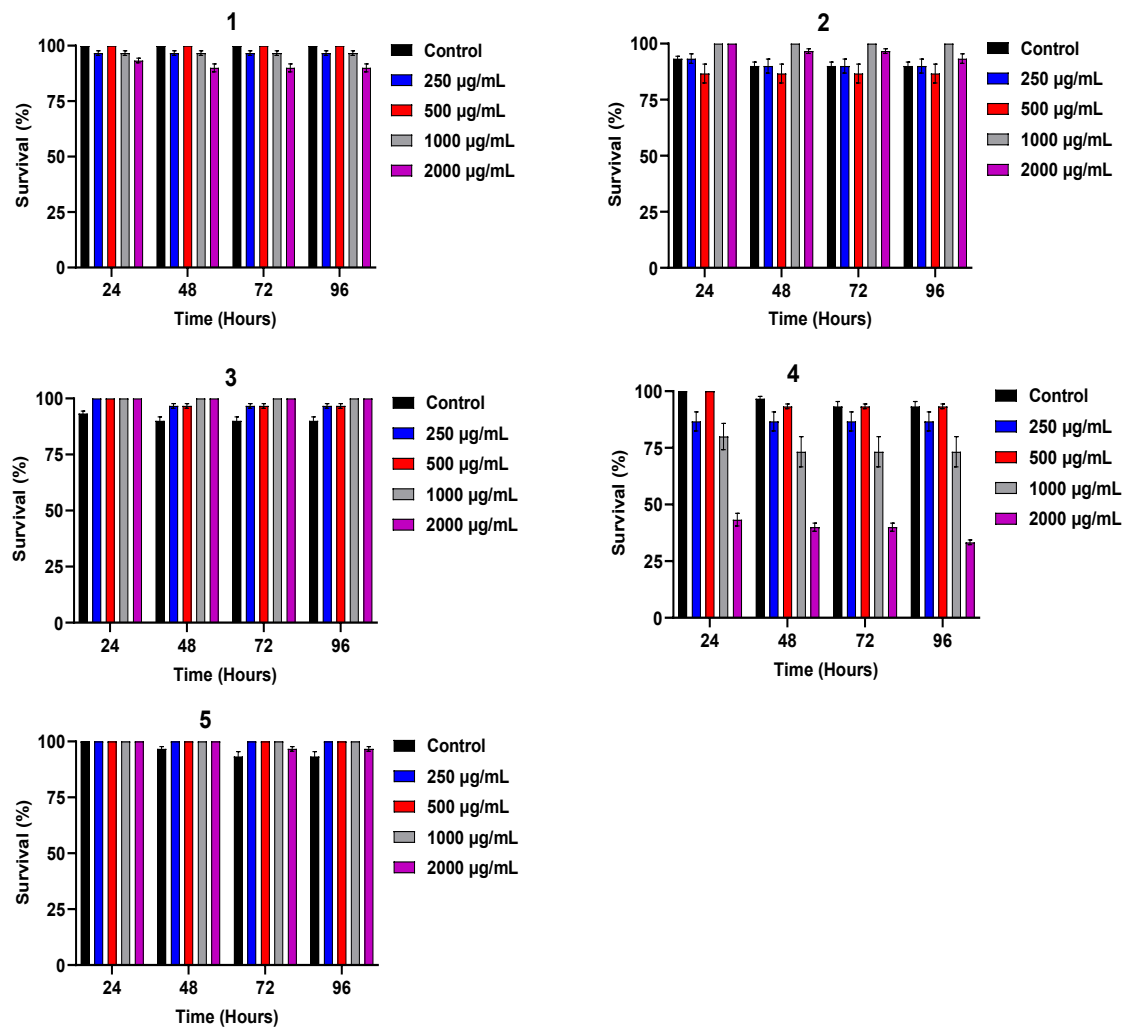


Figure S35. *in vivo* toxicity assays for 1 to 5 against *G. melonella*. GraphPad Prism, n= 3.